Building and Environment 108 (2016) 110–121

Contents lists available at ScienceDirect

Building and Environment

journal homepage: www.elsevier.com/locate/buildenv

Effect of pavement thermal properties on mitigating urban heat islands: A multi-scale modeling case study in Phoenix

Jiachuan Yang [a, *], Zhi-Hua Wang [a], Kamil E. Kaloush [a], Heather Dylla [b]

[a] School of Sustainable Engineering and the Built Environment, Arizona State University, Tempe, AZ 85287, USA
[b] National Asphalt Pavement Association, Lanham, MD 20706, USA

ARTICLE INFO

Article history:
Received 16 June 2016
Received in revised form
15 August 2016
Accepted 20 August 2016
Available online 22 August 2016

Keywords:
Building-environment thermal interactions
CO_2 emission offset
Energy consumption
Outdoor thermal comfort
Pavement
Urban heat island mitigation

ABSTRACT

Engineered pavements cover a large fraction of cities and offer significant potential for urban heat island mitigation. Though rapidly increasing research efforts have been devoted to the study of pavement materials, thermal interactions between buildings and the ambient environment are mostly neglected. In this study, numerical models featuring a realistic representation of building-environment thermal interactions, were applied to quantify the effect of pavements on the urban thermal environment at multiple scales. It was found that performance of pavements inside the canyon was largely determined by the canyon geometry. In a high-density residential area, modifying pavements had insignificant effect on the wall temperature and building energy consumption. At a regional scale, various pavement types were also found to have a limited cooling effect on land surface temperature and 2-m air temperature for metropolitan Phoenix. In the context of global climate change, the effect of pavement was evaluated in terms of the equivalent CO_2 emission. Equivalent CO_2 emission offset by reflective pavements in urban canyons was only about 13.9–46.6% of that without building canopies, depending on the canyon geometry. This study revealed the importance of building-environment thermal interactions in determining thermal conditions inside the urban canopy.

1. Introduction

Urban heat island (UHI), a presence of higher temperatures in an urban area as compared to its rural surroundings, has been considered as one of the major problems in the 21st century [1]. Using satellite-measured surface temperatures, a higher UHI intensity was usually found in summer than that in winter [2]. The adverse effects induced by UHI include but are not limited to, elevated temperatures [3], increased energy consumption [4], air pollution [5], heat-related mortality [6], and disruption to ecosystems [7]. Under the challenge of future climate change, UHI makes cities become unprecedentedly vulnerable to environmental problems that research efforts have been devoted to developing and testing adaptation/mitigation strategies during the past decades [8,9]. Recognized strategies include reflective roofs [10,11], green roofs [12,13], urban vegetation and shading [14–16], heat sinks [17], and cool pavements [18]. Due to the space restrictions in the urban environment, roof material has been extensively studied while pavement material on the ground level has gained limited attention.

Paved surfaces, including roads, parking areas and sidewalks, cover a significant percentage of urban surfaces. A previous study reported that the percentage of paved surfaces ranged from 30 to 39% as seen from above the urban canopy, and from 36 to 45% as seen from under the canopy for a variety of metropolitan areas [19]. With such a significant percentage, modification of pavement materials provides a large potential for mitigating urban heat islands. Though a couple of studies have illustrated the capacity of pavements in reducing UHI and building energy consumption, thermal interactions between buildings and the surrounding microclimate in urban canopies are largely neglected [20]. Different from roof materials, pavement are located inside the urban canyon where buildings substantially alter the heat transport via shading and reflecting radiations. With a three-dimensional building-to-canopy model, Yaghoobian and Kleissl [21] showed that the reflected solar radiation from the reflective pavement can increase annual cooling loads of nearby office buildings by up to 11% in Phoenix. Li [22] conducted an experimental study in Davis, California and observed that around noon on sunny summer days, the

* Corresponding author.
E-mail address: jyang104@asu.edu (J. Yang).

http://dx.doi.org/10.1016/j.buildenv.2016.08.021
0360-1323/

temperature of building walls was 2–5 °C hotter over concrete pavements than over asphalt pavements. Incorporation of the environmental complexity of built terrains is therefore of critical importance in order to provide useful guidance to energy-efficient designs of buildings and paved surfaces, leading to sustainable city planning. In addition, most existing studies have focused on retrofitting pavements with high albedo or reflective construction materials, thus other pavement materials, such as ones with different thermal capacity and conductivity, have been less studied as strategies for UHI mitigation.

Existing studies on the impact of pavements on the urban thermal environment focused on the building-resolving scales and explored offline models where meteorological forcing is provided as boundary conditions [20]. Geographical complexities at city and regional scales, such as spatial heterogeneity, variability in building geometry and density, and local air circulation, are not properly represented. In addition, land-atmosphere interactions are largely neglected in offline models, i.e., meteorological conditions do not respond to changes in building physics. Due to theses limitations, upscaling the results of offline studies for guidance at city and regional scales becomes challenging [23]. Accurate quantification of the effect of pavements on the urban thermal environment necessarily requires studies in a fully-interacting environment, i.e., a coupled atmosphere-urban modeling system.

In this study, the main objective was to evaluate the effect of pavement thermal properties on the urban thermal environment at multiple scales. Towards this end, numerical models were applied with building-environment thermal interactions to: 1) analyze the sensitivity of pavement surface temperature to canyon geometry, 2) identify the impact of pavement thermal properties on the surface temperature, building energy consumption, and outdoor human thermal comfort at a neighborhood scale, and 3) assess the effect of pavement thermal properties in mitigating UHI at a regional scale. The metropolitan Phoenix in Arizona was selected as the testbed because of the rapid urbanization in the past decades which has created a significant UHI in this region. The equivalent CO_2 emission offset by reflective pavement due to modified radiative forcing at the global scale was also estimated and discussed.

2. Numerical tools and study area

This section describes the numerical tools used to investigate impacts of pavements in the built environment in this study. An offline (stand-alone) urban canopy model was adopted for studying the impact at the neighborhood scale. The offline model is suitable for long-term simulations at the neighborhood scale due to its high computational efficiency. However, land-atmosphere interactions are largely neglected in the offline model. At the city and regional scales, an online (coupled) Weather Research and Forecasting (WRF)-Urban modeling system was used to account for the land-atmosphere interactions and surface heterogeneity. Nevertheless, the requirement of high-performance computational resources imposes constraints on spatial resolution and simulation time of online models.

2.1. Urban canopy model

To accurately quantify the impact of pavements in the built environment, a numerical model that captures coupled urban energy and water budgets is needed. Here a state-of-the-art urban canopy model (UCM) [24,25] was used. The UCM represents building arrays as a two-dimensional street canyon, as illustrated in Fig. 1(a). The model features a realistic representation of hydrological processes over natural and engineered surfaces, sub-facet heterogeneity, building-environment thermal interaction in the canyon, and analytical solutions to heat transfer in building envelopes. Model performances over various pavement surfaces in the urban area have been validated by in-situ measurements under different climate conditions [25,26]. Detailed computational processes of the model can be found in the original paper and thus are not duplicated here.

2.2. WRF-urban modeling system

During the past decades, a growing concern on urban heat island has led to development of numerous mesoscale atmosphere-urban modeling systems [27–29]. Among the developed systems, one powerful tool is the WRF-Urban modeling system, which has been widely utilized and examined for major metropolitan regions around the world [30–32]. In this study the developed urban canopy model was implemented into the WRF model version 3.4.1 and the new model was employed to access the impact of pavements at the regional scale. Initial meteorological conditions for the WRF simulations were obtained from the National Centers for Environmental Prediction Final Operational Global Analysis data, which were available on a $1^\circ \times 1^\circ$ resolution with a 6-h temporal frequency (details can be found on http://rda.ucar.edu/datasets/ds083.2/). Land use information was acquired from the National Land Cover Database (NLCD) 2006 [33].

2.3. Study area

For the urban canopy model, meteorological measurements in the atmospheric boundary layer are required as model inputs. Observations obtained from the eddy-covariance flux tower deployed at Maryvale, west Phoenix (see Fig. 1(b)) were used to drive offline simulations. The experimental site is a high-density residential area with single-family houses with a mean lot size of about 700 m^2 [34]. Generally, the daily mean incoming shortwave radiation is greater than 600 W m^{-2} and the daily mean air temperature at 22 m is higher than 30 °C in summer. The monsoon season starts June 29 and ends September 30. The wind speed in the study area is about 3 m s^{-1} in summer, with a prevailing wind direction towards the west [34].

3. Effect of canyon geometry

Urban geometry plays a crucial role in determining the magnitude of shading and trapping effects that its impact on pavement surface temperature needs to be addressed [35]. In this section the sensitivity of pavement surface temperature to canyon geometry was analyzed with the urban canopy model. Capability of the model in reproducing energy and water budgets of the study residential area at the annual scale (year 2012) was verified in a previous study [36]. The calibrated parameters were summarized in Table 1 and were used for subsequent offline numerical simulations. As reflective pavement has gained increasing popularity recently, it was used as an example to illustrate the effect of canyon geometry. Focusing on the time when the urban thermal environment is extremely aggravated, numerical simulations were carried out for a pre-monsoon summer period, 12–17 June 2012, when high temperatures were observed under clear sky conditions. Pavements were modeled with an albedo (the ratio of reflected radiation from the surface to incident radiation upon it) of 0.1, 0.3, 0.5 and 0.7, while other thermal properties remained the same as shown in Table 1. The first set of simulation modeled a pavement surface without canopy (e.g., open ground space, parking lot), while the second set simulated a pavement surface in the canyon of a typical high-density residential area.

Averaged diurnal profiles of pavement surface temperature are

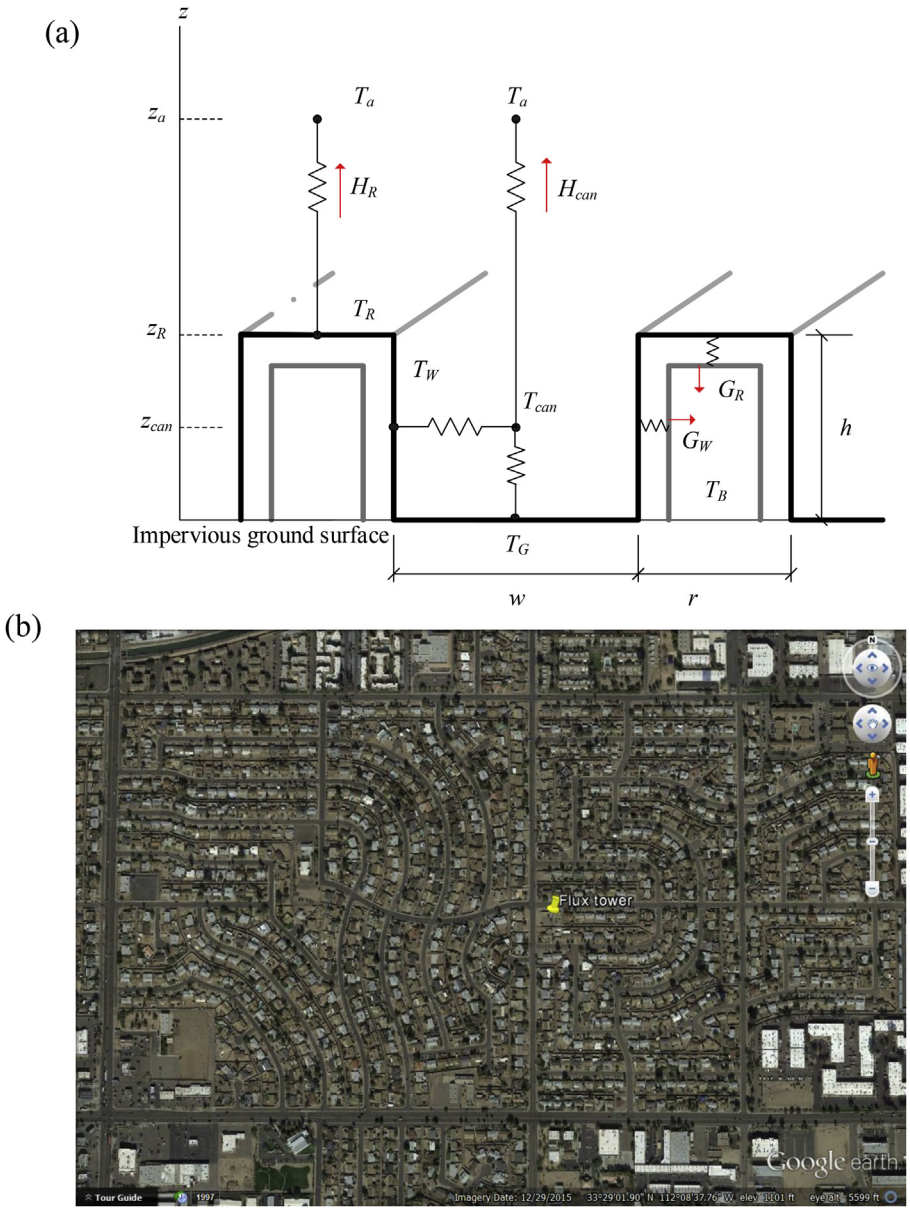

Fig. 1. (a) Schematic of the urban canopy model: *h*, *w*, and *r* are the normalized building height, canyon width, and building width, respectively; H is the sensible heat flux, G is the storage heat flux, *T* is the temperature, *z* is the height, subscripts *R*, *W*, *G*, *can*, *a*, *B* denote properties of roof, wall, ground, canyon, air and building. (b) Location of the flux tower in a high-density residential area in Phoenix (Google Earth basemap).

Table 1
Input parameters for a residential area in Phoenix using the urban canopy model.

Input parameters	Symbol	Values	Input parameters	Symbol	Values
Latitude (degree)	*Lat*	34.42	Normalized building height	*h*	0.5
Longitude (degree)	*Lon*	111.93	Normalized canyon width	*w*	0.5
Emissivity of ground (–)	ε_G	0.95	Heat conductivity of ground (W m^{-1} K^{-1})	k_G	0.9
Emissivity of wall (–)	ε_W	0.95	Heat conductivity of wall (W m^{-1} K^{-1})	k_W	1.3
Emissivity of roof (–)	ε_R	0.95	Heat conductivity of roof (W m^{-1} K^{-1})	k_R	1.2
Albedo of ground (–)	a_G	0.1	Heat capacity of ground (MJ m^{-3} K^{-1})	C_G	2.1
Albedo of wall (–)	a_W	0.2	Heat capacity of wall (MJ m^{-3} K^{-1})	C_W	1.5
Albedo of roof (–)	a_R	0.1	Heat capacity of roof (MJ m^{-3} K^{-1})	C_R	1.9
Thickness of wall (m)	d_W	0.18	Roughness length above roof (m)	$Z_{m,R}$	0.01
Thickness of roof (m)	d_R	0.3	Roughness length above ground (m)	$Z_{m,G}$	0.05
Canyon orientation	θ_{can}	π/8			

shown in Fig. 2. Fig. 2 shows that increasing pavement albedo significantly reduced surface temperature in the absence of canopy. With an increase of 0.6 in surface albedo, daily peak pavement surface temperature decreased about 23 °C in average in the

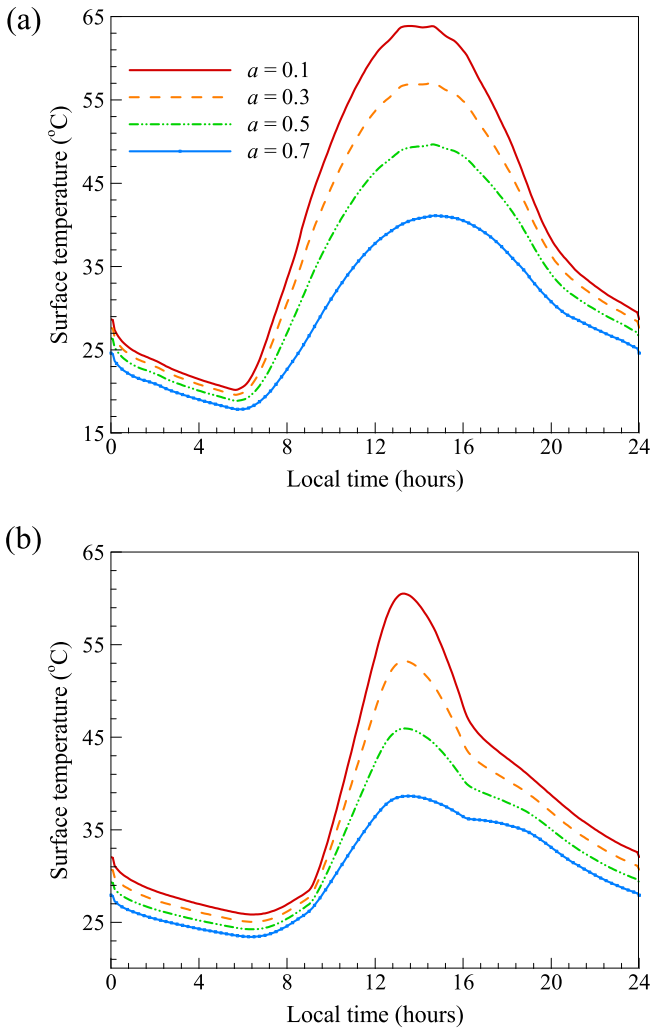

Fig. 2. Averaged diurnal profiles of predicted pavement surface temperatures with different albedo (a) without a canopy, and (b) in a high-density residential area in Phoenix during 12–17 June 2012.

simulation period. With the canopy, the reflective material was also able to reduce pavement surface temperature considerably, with a daily peak cooling effect of about 20 °C. However, adjacent buildings blocked part of the incoming solar radiation for the pavement and therefore the albedo was less effective inside the street canyon. Without canopy, temperature difference between pavements with different albedo increased rapidly after sunrise at around 0530 local time. Increasing albedo from 0.1 to 0.7 reduced pavement surface temperature by more than 10 °C for about 11 h. On the other hand, the albedo modification did not cool pavement surface significantly until about 0930 local time with the canopy, when pavement started to become not fully shaded by adjacent buildings. Cooling effect of more than 10 °C only lasted for about 5 h, which was less than half of that without canopy. During nighttime, albedo of materials became ineffective due to the absence of solar radiation. However, as more radiation was reflected and less thermal energy was stored during the day, reflective pavement led to a reduction of about 3 °C in nighttime surface temperature both with and without canopy. It is noteworthy that the nighttime surface temperature of pavement was higher with the canopy due to radiative trapping. Buildings absorbed outgoing longwave radiation from pavement and emitted longwave radiation back. Thermal energy was thus trapped inside the urban canyon that heat storage in the pavement during the day was dissipated slowly.

A third set of simulation was carried out to quantify the effect of canyon aspect ratio (h/w) and canyon orientation (θ_{can}) on pavement surface temperature. In the simulation the albedo of pavement was increased from 0.1 to 0.7 with varying canyon aspect ratios and orientations, while other parameters remained the same as shown in Table 1. Fig. 3(a) presents the averaged diurnal profiles of surface temperature reduction by increasing pavement albedo from 0.1 to 0.7 with different canyon aspect ratios ($\theta_{can} = \pi/8$). It suggested that cooling effect of reflective pavement decreased with aspect ratio. Daily peak temperature reduction by reflective pavement was about 27 °C with an aspect ratio of 0.5, and became around 14 °C when h/w equaled to 4. In a deeper street canyon (large h/w value), shading effect of buildings dominates that pavement receives incoming solar radiation only around noon time. Under this condition, the effective period of the reflective pavement is significantly reduced. For example, with an aspect ratio of 4, the cooling effect by the reflective pavement was larger than 4 °C only for the period from 1200 to 1530 local time. The impact of canyon orientations is shown in Fig. 3(b) ($h/w = 1$). Changing the canyon orientation θ_{can} modified the pattern of diurnal variation of the cooling effect. For the study area in Phoenix, diurnal profile of the cooling effect with $\theta_{can} = \pi/8$ was almost identical to that with

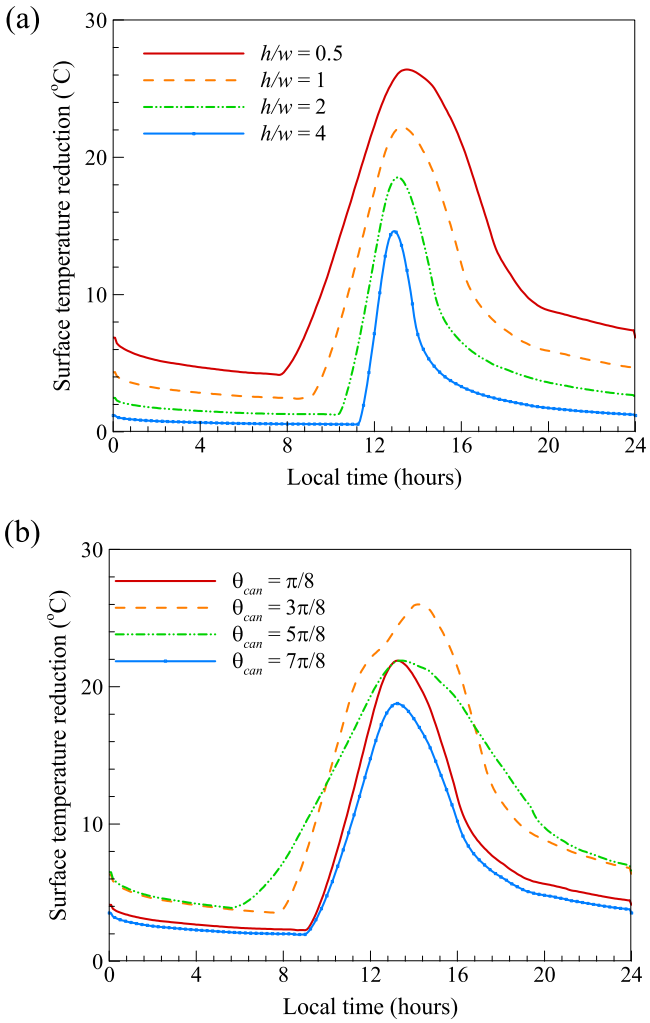

Fig. 3. Averaged diurnal profiles of surface temperature reductions by increasing the pavement albedo from 0.1 to 0.7 with different (a) aspect ratios ($\theta_{can} = \pi/8$), and (b) canyon orientations ($h/w = 1$) in Phoenix during 12–17 June 2012.

$\theta_{can} = 7\pi/8$, except that the magnitude was consistently smaller. The efficient period of the reflective pavement (cooling > 5 °C) with $\theta_{can} = 5\pi/8$ was substantially longer than that with $\theta_{can} = \pi/8$, though the peak cooling effect was close. Among the studied canyon orientations, the maximum daily peak temperature reduction was observed with $\theta_{can} = 3\pi/8$, which was about 7 °C greater than that with $\theta_{can} = 7\pi/8$. Results indicated that when deployed inside a street canyon, the performance of reflective pavements is largely determined by canyon geometry.

4. Impact of pavements at a neighborhood scale

4.1. Surface temperature

To identify the importance of building-environment thermal interactions in the urban canyon, in this section the effect of pavements on the road and wall surface temperatures in Phoenix was investigated. The sunny pre-monsoon period studied in section 3, 12–17 June 2012, was used for this section. To illustrate the maximum effect of pavements, it was assumed that the road surface was 100% pavement with no trees or vegetation. For subsequent analysis in this section, an aspect ratio of 1 and a canyon orientation of 0 were used for the study neighborhood.

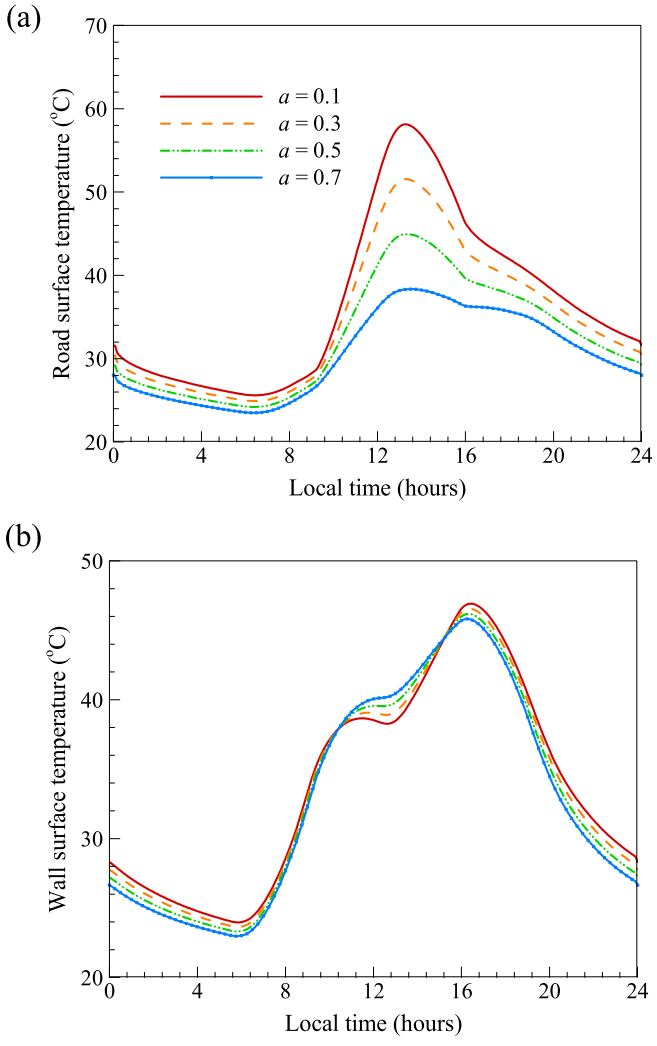

Fig. 4. Simulated (a) road surface temperatures, and (b) wall surface temperatures with different surface albedo for the pavement in Phoenix during 12–17 June 2012.

Fig. 4(a) illustrates that increasing pavement albedo cooled the road surface considerably. An increase of 0.6 in albedo led to a pavement surface temperature reduction of up to about 20 °C in daytime. With reduced road surface temperatures, the reflective pavement emitted less longwave radiation to the canyon environment. Nevertheless, more shortwave radiation was reflected that the combined effect of the reflective pavement was complicated. Fig. 4(b) shows that across the diurnal cycle, increasing pavement albedo resulted in a warming effect on building walls from around 1030 to 1500 local time. The increased wall temperature indicated that reflected shortwave radiation outweighed reduced longwave radiation from the reflective pavement during this period. In the rest of the diurnal cycle, the reflective pavement led to cooling of wall surface temperatures. The maximum warming effect of about 2.0 °C was observed at 1330 local time, while the maximum cooling effect of about 1.9 °C occurred at 2100 local time. Note that the daytime warming effect may increase the peak electricity load and cooling demand of the building, which is unfavorable for cities especially in summers. In terms of nighttime cooling, it saves cooling demands in hot seasons. However, it may cause additional heating demands in cold seasons.

Performance of pavements depends on a number of thermal properties, among those albedo is an important but not the only determinant one. Pavements with high porosity, heat capacity, and thermal conductivity have also been studied as strategies for UHI mitigation [18]. Pavement with high thermal conductivity, and pavement with large heat capacity were studied here as alternative strategies for Phoenix urban heat island. Three simulations were conducted with different values assigned to both thermal properties. For thermal conductivity, the studied values were 1.2, 2.0, and 3.0 W K^{-1} m^{-1}, respectively. Tested heat capacities were 1.4, 2.0, and 2.8 MJ K^{-1} m^{-3}.

Results of thermal conductivity are plotted in Fig. 5. Fig. 5(a) illustrates that increasing thermal conductivity led to lower road surface temperatures during daytime for Phoenix, as a large thermal conductivity favored the transfer of radiative energy into the pavement. On the other hand, during the nocturnal cycle, heat released from the pavement due to a large thermal conductivity increased the road surface temperature. This indicated that the diurnal variation of road surface temperatures increased with the rate of heat transfer process in the pavement. With an increase of 1.8 W K^{-1} m^{-1} in the thermal conductivity, maximum daytime reduction and nighttime increment of the road surface temperature were about 7.0 and 2.4 °C, respectively. In terms of the wall surface temperature, modifying the thermal conductivity of ground pavement had a relatively insignificant impact. Maximum cooling and warming effects were about 1.0 and 1.3 °C, respectively.

The effect of heat capacity is shown in Fig. 6, which was similar to the result of thermal conductivity. Enabling ground pavements to store more energy, a large heat capacity tended to reduce the daytime peak road surface temperature. The stored energy was released at night and led to a heating of the road surface. When the heat capacity of ground pavements was doubled from 1.4 to 2.8 MJ K^{-1} m^{-3}, maximum daytime reduction and nighttime increment of the road surface temperature were about 5.7 and 2.2 °C for Phoenix. With respect to the wall surface temperature, modifying the heat capacity of ground pavement led to insignificant cooling and warming effects of up to 1.0 and 0.9 °C. Simulation results in this section illustrated that modifying the thermal properties of pavements had a limited impact on the wall surface temperature, even during the hot summer of a year in a desert city.

4.2. Building energy consumption

After realizing the effect of different pavement thermal

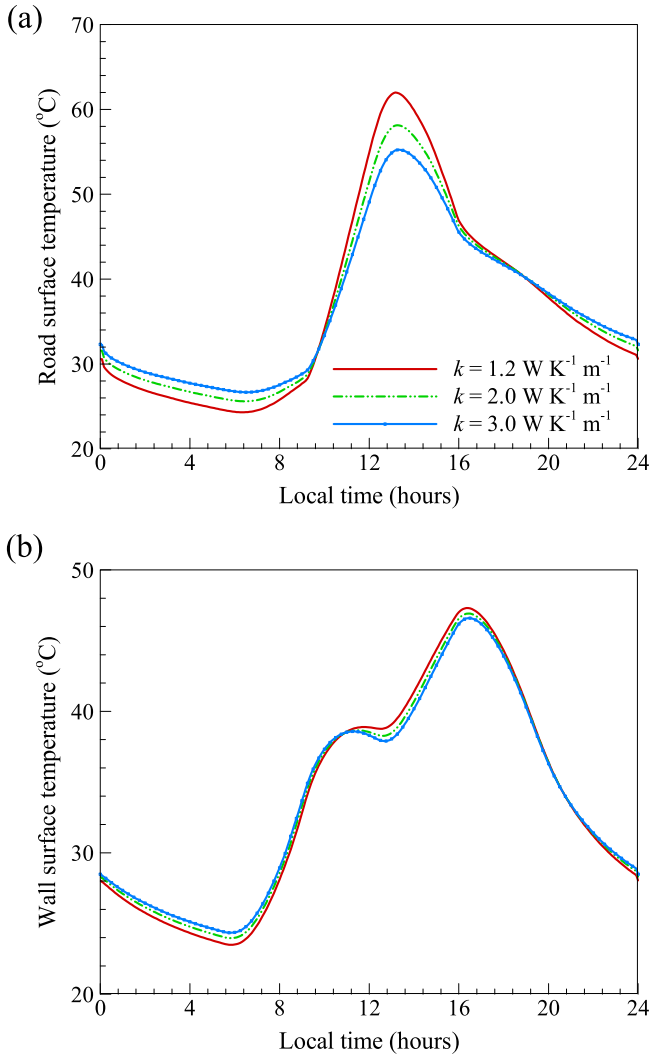

Fig. 5. Simulated (a) road surface temperatures, and (b) wall surface temperatures with different thermal conductivity for the pavement in Phoenix during 12–17 June 2012.

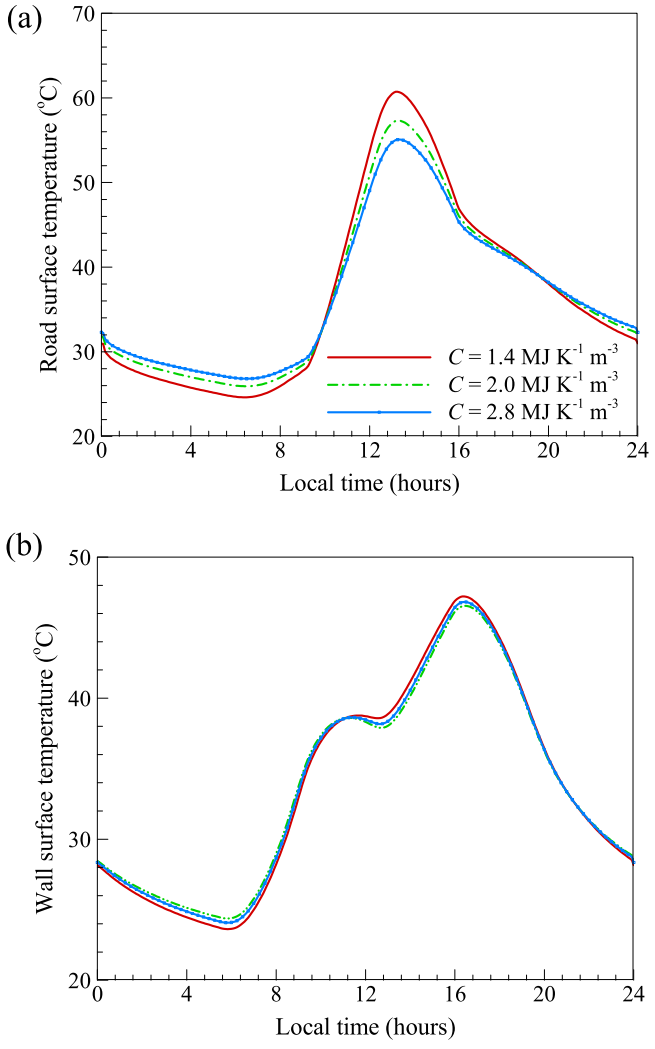

Fig. 6. Simulated (a) road surface temperatures, and (b) wall surface temperatures with different heat capacity for the pavement in Phoenix during 12–17 June 2012.

properties on surface temperatures in the urban canyon, a series of simulation was carried out to access the impact of pavement thermal properties on the building energy consumption. Using the calibrated UCM, the effect of pavement thermal properties on the building energy consumption was tested at the annual scale. To illustrate the effect of same materials on different urban facets, simulations were conducted separately for roof and ground surfaces. Insulation was not considered in this study, which may lead to an overestimation of the building energy consumption. For ground and roof surfaces, four cases were studied. Thermal properties of the material in each case were (1) control case: $a = 0.1$, $k = 1.2$ W K^{-1} m^{-1}, $C = 1.4$ MJ K^{-1} m^{-3}; (2) reflective material: $a = 0.5$, $k = 1.2$ W K^{-1} m^{-1}, $C = 1.4$ MJ K^{-1} m^{-3}; (3) material of low thermal conductivity: $a = 0.1$, $k = 0.6$ W K^{-1} m^{-1}, $C = 1.4$ MJ K^{-1} m^{-3}; and (4) material of large heat capacity: $a = 0.1$, $k = 1.2$ W K^{-1} m^{-1}, $C = 2.8$ MJ K^{-1} m^{-3}. These values were within the typical range of engineering materials documented in the literature. The thickness of materials for roof, wall, and ground were 0.3, 0.18, and 0.45 m, respectively.

Following previous studies [36,37], the building energy consumption was estimated based on the heat flux entering the building through the innermost layer of the wall and the roof, given by:

$$Q_{in} = \frac{k(T_{in} - T_B)}{d_{in}/2}, \quad (1)$$

where Q_{in} is the heat flux entering the building via wall or roof, d_{in} and T_{in} are the thickness and temperature of the innermost (discrete) layer, T_B is the building indoor temperature. With this equation, the estimated energy consumption mainly considers the sensible load of buildings that the latent load is largely ignored. In addition, two factors are neglected: (1) the internal energy loads caused by people and equipment, and (2) the efficiency of air conditioning system and the variation of the building indoor temperature. Note that heat fluxes into the building through roof and wall via conduction were calculated separately in the UCM. As U.S. Department of Energy suggested that the thermostat should be set to around 25.6 °C for indoor thermal comfort [38], the building indoor temperature was assumed to be maintained at 25 °C by indoor heating, ventilation, and air-conditioning (HVAC) systems for the entire simulation period.

Fig. 7 presents the monthly energy consumption of the building in a residential area in Phoenix. Total annual energy consumptions due to the heat conduction via roof and wall with different

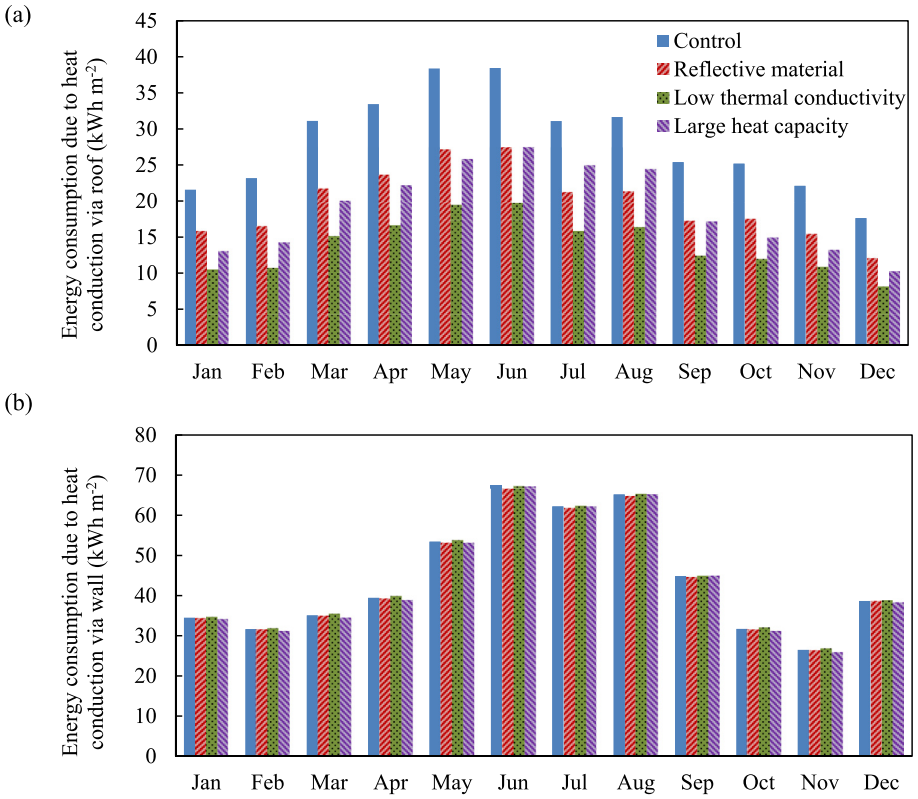

Fig. 7. Monthly energy consumption of buildings due to heat conduction via (a) roof, and (b) wall with different engineering materials for Phoenix in 2012.

materials were summarized in Table 2. Note that in the UCM, the rooftop is not thermally interacted with the street canyon. Therefore Fig. 7(a) represents the effect of various roof materials on the building energy consumption, and Fig. 7(b) illustrates the impact of pavement materials. In terms of the roof surface, Fig. 7(a) indicates that the material of low thermal conductivity was the most efficient in reducing building energy consumptions. As it slowed the heat exchange across the building envelope, energy consumptions were substantially reduced throughout the year. Total annual energy consumptions decreased by about 50% as compared to the control case. Increasing albedo and heat capacity of the roof material also led to evident savings of energy consumptions. In cool to cold periods, the reflective material yielded greater energy consumptions than those with a large heat capacity, primarily due to the resulted heating penalty at nighttime. Whereas in summers, warming effects from the material of large heat capacity caused extra cooling demands at night, and the reflective material was more effective in saving building energy consumptions. At the annual scale, increasing the heat capacity of the roof material was more efficient in enhancing the building energy efficiency than increasing albedo for the study area. Compared to deployment of reflective materials, using materials of large heat capacity for the roof surface saved total annual energy consumptions by about 9 kWh m^{-2}. This result emphasizes the previous finding that the thermal performance of materials is determined by multiple parameters, benefits of various mitigation strategies should be compared to come up with the best solution [39].

Fig. 7(b) shows that energy consumptions due to the heat conduction via wall was significantly larger than that via roof, mainly due to the difference in the thickness of materials; however, among studied thermal properties, it was found that modifying ground pavements had negligible effects on the building energy consumption. Note that the unit of energy consumptions is kWh per square meter of wall surface facing the sun. Total annual energy savings in different cases were very small, ranging from −20 to 7 kWh m^{-2}, which was less than 3% of the annual energy consumption in the control case. Note that the material of low thermal conductivity on roof substantially reduced building energy consumptions, however, it slightly increased the energy consumption of adjacent buildings when deployed at the ground level. The results illustrate that the same engineering material may lead to an opposite effect on the building energy efficiency when applied to different urban spatial locations.

4.3. Outdoor thermal comfort

Under the semi-arid climate, residents experience intense thermal discomfort during hot days in outdoor or non-air-

Table 2
Summary of thermal properties and total annual energy consumptions in different simulation cases for Phoenix in 2012.

	Control case	Reflective material	Material of low thermal conductivity	Material of large heat capacity
Albedo	0.1	0.5	0.1	0.1
Thermal conductivity (W K^{-1} m^{-1})	1.2	1.2	0.6	1.2
Heat capacity (MJ K^{-1} m^{-3})	1.4	1.4	1.4	2.8
Total annual energy consumption through roof (kWh m^{-2})	339	238	168	228
Total annual energy consumption through wall (kWh m^{-2})	727	707	734	719

conditioned indoor environments in metropolitan Phoenix [40]. High temperature significantly increases the risk of heat-related morbidity and mortality in cities, especially under the challenge of global warming [41]. Close to pedestrians on the street level, pavements play a dominant role on outdoor human thermal comfort. Quantifying thermal comfort in outdoor urban areas can be a challenging process, due to the variety of environmental factors, including temperature, humidity, wind speed, radiative exposure, ambient evaporative, and sensible fluxes [42]. The Index of Thermal Stress (*ITS*) developed by Givoni [43] was chosen to assess the impact of pavements on outdoor thermal comfort for Phoenix:

$$ITS = [R_n + C + (M - W)]/f, \quad (2)$$

where R_n is the body's net radiation, C is the convective energy exchange, M is the heat generated by body's metabolism, W is the heat consumed through work, and f is the efficiency of sweat evaporation. All variables in Equation (2) has the unit of W m^{-2} except the dimensionless variable f. The *ITS* is a measure of the rate at which the human body must secrete sweat to maintain thermal equilibrium. It accounts for human metabolism, mechanical work, radiation exchange, clothing condition, wind speed, humidity, and temperature. By definition, outdoor thermal comfort decreases with the *ITS*.

In this study, we assumed a pedestrian was performing mild outdoor activities (e.g., walking) with light summer clothing in the street canyon. In total four cases were studied for the simulation period of 12–17 June 2012. Thermal properties of the pavement surface in each case were the same as those listed in Table 2. Increase of the *ITS* by different pavements as compared to the control case for the entire simulation period is presented in Fig. 8. Fig. 8 clearly demonstrates that modifying the thermal conductivity and heat capacity of pavements had negligible impacts on outdoor human thermal comfort across the diurnal cycle. On the other hand, with increased solar reflection, the reflective pavement significantly increased the thermal stress on pedestrians, up to more than 100 W m^{-2} around noontime throughout the simulation period. This finding was in agreement with recent studies where the reduced surface temperature was found not enough to offset increased radiation loads from reflective pavements [44]. In nighttime, the effect of reflective pavements was insignificant as solar radiation was not available.

4.4. Regional effect of pavements

To incorporate the impact of land-atmosphere interaction and land surface heterogeneity, we adopted the coupled WRF-UCM modeling system to quantify the regional effect of pavements for metropolitan Phoenix. Following a previous study's setup [13], we used an inner domain of 212 km × 212 km to cover metropolitan Phoenix with a spatial resolution of 2 km. Detailed experimental set-up of the WRF-UCM modeling system is referred to the previous study [13]. Due to the limitation of time and computational resources, the simulation period was set to be 1–11 July 2006. Using the 2006 NLCD land cover data, the urban land-use was divided into three categories: low-density residential, high-density residential, and industrial and commercial. The performance of the WRF model against field observations from ground-based weather stations for Phoenix has been verified [13]. The calibrated parameters for each land-use category were summarized in Table 3. Thermal properties of pavements in four studied cases were the same as those listed in Table 2 except that the pavement albedo was 0.17 in the control case. Pavement properties were changed for all three urban categories in the simulation. Simulated impact of the reflective pavements on land surface temperature (T_s) and 2-m air temperature (T_2) at 1400 local time is shown in Fig. 9. As shown in Fig. 9, increasing the albedo of pavement surfaces from 0.17 to 0.5 led to a cooling effect of less than 0.5 °C for Phoenix. This temperature reduction was insignificant given that the surface temperature was higher than 45 °C at 1400 local time in Phoenix, and was significantly smaller than the predicted reduction from offline simulations. With limited cooling impacts on urban land surface, the reflective pavement had negligible influences on 2-m air temperature.

Simulated impact of the pavements with large heat capacity and low thermal conductivity on land surface temperature for Phoenix are plotted in Fig. 10. Increasing the heat capacity resulted in a lower pavement surface temperature, and the pavement of reduced thermal conductivity led to an elevated surface temperature. The magnitude of temperature change in both cases was less than 0.5 °C, indicating a limited effect of the pavements on land surface temperature. In terms of 2-m air temperature, the effect of both pavements was also negligible (results not shown here).

Online simulation results were qualitatively similar to offline findings. However, the magnitude of the temperature change from online simulations was substantially smaller than that predicted by the offline model. The principal reason was that land surface temperature from the WRF-UCM modeling system was a lumped average over all urban surfaces including road, wall, and roof. Existence of bare soil and vegetative surface in urban areas further attenuated the impact of pavements, which could be up to 35% in low-density residential areas as shown in Table 3. After accounting for the land-atmosphere interaction and land surface heterogeneity, modifying the thermal properties of pavements was found to have a limited effect on urban land surface temperature and air temperature for Phoenix at the regional scale.

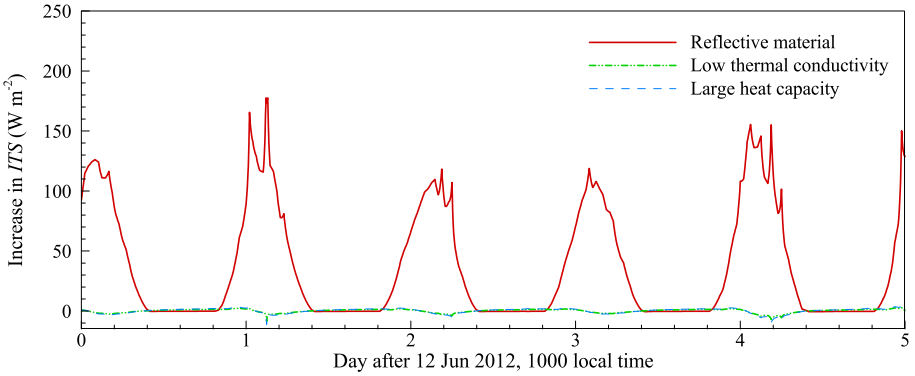

Fig. 8. Increase in *ITS* of a pedestrian in the street canyon by different pavements during 12–17 June 2012 for Phoenix.

Table 3
Summary of input parameters for different urban-land categories in the WRF-Urban modeling system for metropolitan Phoenix.

Input parameters	Unit	Industrial and commercial	High-density residential	Low-density residential
h (building height)	m	17.0	7.5	5.0
l_{roof} (roof width)	m	10.0	9.4	8.3
l_{road} (road width)	m	10.0	9.4	8.3
f_{urb} (urban fraction)	–	0.95	0.85	0.65
a_R (albedo of roof)	–	0.15	0.16	0.16
a_W (albedo of wall)	–	0.15	0.16	0.16
a_G (albedo of ground)	–	0.17	0.17	0.17
C_R (heat capacity of roof)	MJ K^{-1} m^{-3}	1.35	1.35	1.35
C_W (heat capacity of wall)	MJ K^{-1} m^{-3}	1.35	1.35	1.35
C_G (heat capacity of ground)	MJ K^{-1} m^{-3}	1.4	1.4	1.4
k_R (thermal conductivity of roof)	W K^{-1} m^{-1}	0.70	0.70	0.70
k_W (thermal conductivity of wall)	W K^{-1} m^{-1}	0.70	0.70	0.70
k_G (thermal conductivity of ground)	W K^{-1} m^{-1}	1.2	1.2	1.2

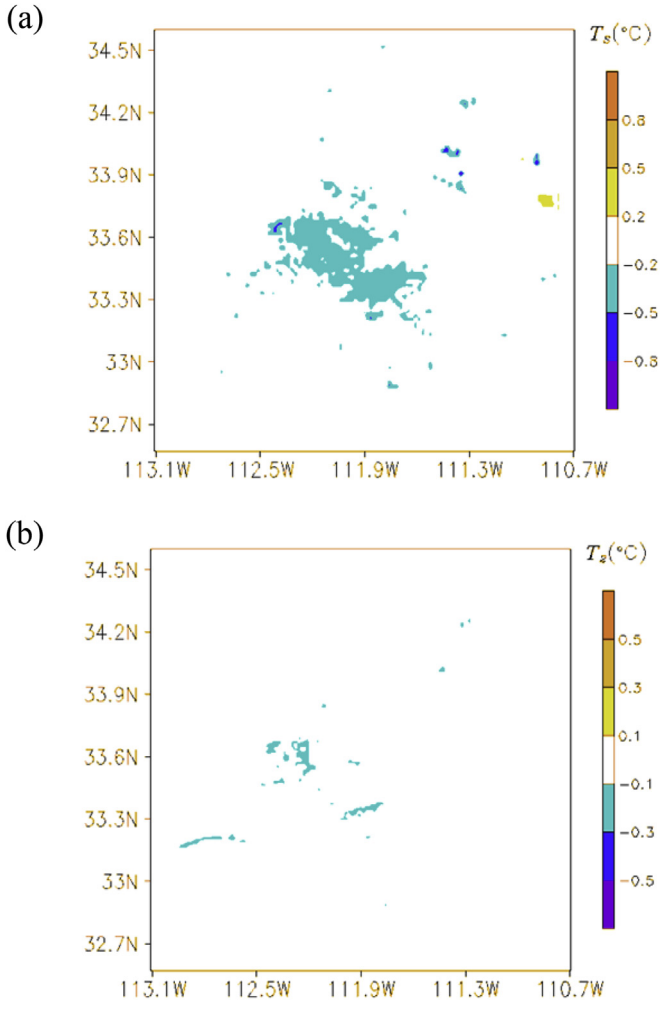

Fig. 9. Simulated impact of the reflective pavement on (a) land surface temperature, and (b) 2-m air temperature at 1400 local time for Phoenix.

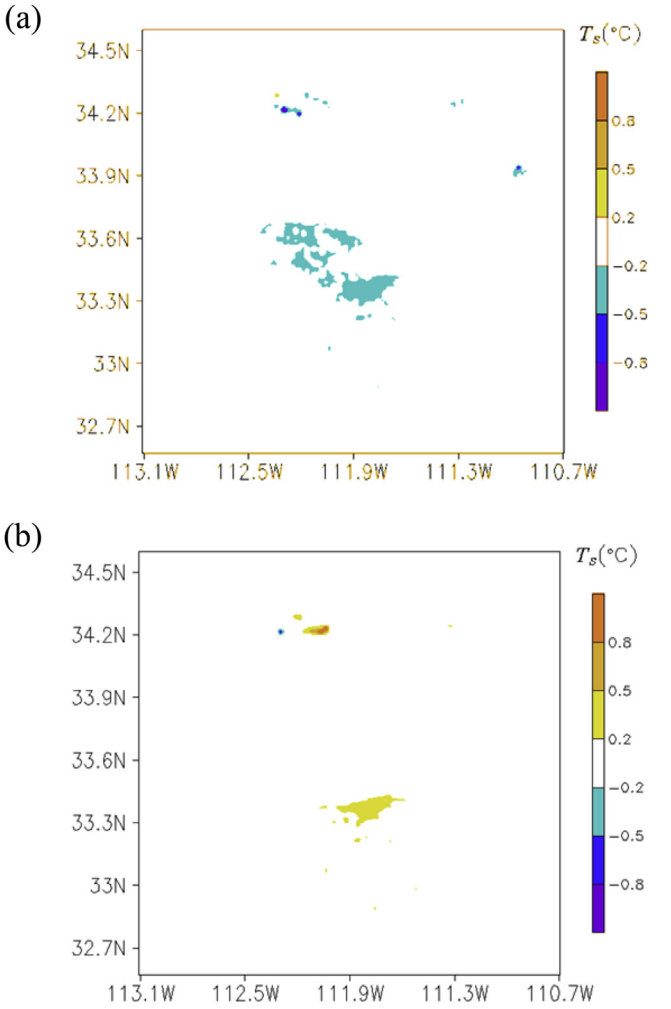

Fig. 10. Simulated impact of (a) the pavement of large heat capacity and (b) the pavement of low thermal conductivity on land surface temperature at 1400 local time for Phoenix.

5. CO_2 emission offset

At the global scale, the ultimate goal of comparing effects of different pavements is to determine the efficient material for countering global warming. A previous study [45] reported that a net albedo increase of about 0.1 in global urban areas could induce a negative radiative forcing on the earth equivalent to a one-time offsetting 44 Gt of CO_2 emissions. 40% of the emission offset (20 Gt) was achieved by modifying pavement albedo, and the rest 60% (24 Gt) was accomplished through reflective roofs. Nevertheless, the neglect of thermal interactions inside the urban canyon raises uncertainty for their findings. The UCM used in this study also enables a more realistic estimate of the effect of pavements in terms of CO_2 emission offset. As heat capacity and thermal conductivity have no impact on shortwave radiation budgets, only

reflective pavements were studied in this section.

The net shortwave radiation budgets over road and wall surfaces inside the urban canyon are given by:

$$S_W = (1 - a_W)\left(\frac{l_{shadow}}{2h} + \frac{w - l_{shadow}}{w} a_G F_{WG} + \frac{l_{shadow}}{2h} a_W F_{WW}\right) S^{\downarrow}, \quad (3)$$

$$S_G = (1 - a_G)\left(\frac{w - l_{shadow}}{w} + \frac{l_{shadow}}{2h} a_W F_{WW}\right) S^{\downarrow}, \quad (4)$$

where S is the net shortwave radiation and $S^{\downarrow}$ is the download incoming shortwave radiation; subscripts 'W' and 'G' denote wall and ground respectively; l_{shadow} is the normalized shadow length; F_{WG} and F_{WW} are the sky view factors between wall and ground, and between wall and wall, respectively, calculated as:

$$F_{WW} = \sqrt{1 + \left(\frac{w}{h}\right)^2} - \frac{w}{h}, \quad (5)$$

$$F_{WG} = 0.5(1 - F_{WW}). \quad (6)$$

Equations (2)–(5) suggest that the magnitude of outgoing shortwave radiation varies with urban geometry, albedo of ground and wall surfaces, and normalized shadow length. Thus the sensitivity of reflected radiation (from urban canopy to overlying atmosphere) to urban geometry and pavement albedo was investigated for the Phoenix metropolitan area in this section. Other parameters were obtained from Table 1.

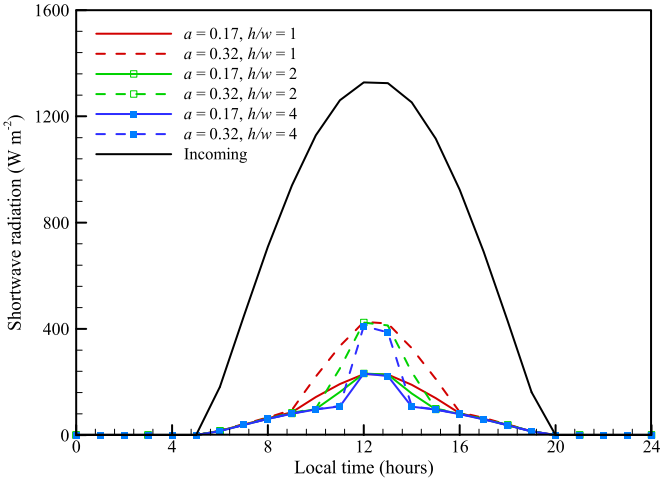

Fig. 11. Diurnal profiles of incoming and reflected shortwave radiation for pavements with different albedo in Phoenix urban canyon on the summer solstice day, 2012.

Note that the normalized shadow length varies with the solar azimuth angle and zenith angle, therefore the resultant effect of reflective pavements has diurnal and seasonal variations. Following the previous study [45], a 0.15 increase in pavement albedo was assumed for the Phoenix metropolitan area. Diurnal profiles of incoming and reflected shortwave radiations for pavements with different canyon aspect ratios are shown in Fig. 11 for the summer solstice day, where a large variability was observed. After sunrise, the albedo of pavement surface began to function by reflecting the reflected shortwave radiation from building walls. As the sun continued to rise, pavements began to receive both direct incoming shortwave radiation from the sun and reflected shortwave radiation from walls. During this period pavement albedo became efficient because direct incoming shortwave radiation was significantly larger than reflected shortwave radiation from walls. Around noontime when the sun was directly overhead, pavements received only direct incoming shortwave radiation from the sun that the impact of pavement albedo inside the urban canopy was similar to that of an open space without canopy in terms of radiative heat exchange. Despite variations of the canyon aspect ratio, a 0.15 increase in pavement albedo increased the reflected shortwave radiation by about 180 W m^{-2} around noontime for all cases. Depending on the canyon aspect ratio, the efficient period of reflective pavement ranged from 3 h to 7 h.

To identify the seasonal variation of the impact of reflective pavements on urban shortwave budgets, we employed an index named daily effective albedo. Daily effective albedo is defined as the ratio between total reflected shortwave radiation and total incoming shortwave radiation over an urban canyon across the diurnal cycle. Compared to the material (nominal) albedo, the daily effective albedo is more appropriate for accessing the effect of pavements on urban radiation budgets as it accounts for thermal interaction and geometry effect in cities. Variations of the daily effective albedo for pavements in urban canyons with different aspect ratios is plotted in Fig. 12 for year 2012. Fig. 12 shows that the daily effective albedo had a larger seasonal variation in a deeper canyon. Averaging over the entire year 2012, an increase of 0.15 in pavement albedo resulted in an increase of 0.070, 0.045, and 0.021 in the daily effective albedo when h/w equaled to 1, 2, and 4, respectively. These values were used for calculating the effect of reflective pavements on CO_2 emission offset at the global scale.

Following the methodology used by Akbari et al. [45], the change in radiative forcing is −1.27 W m^{-2} per 0.01 increase in the albedo of global land surface. Considering a global paved surface

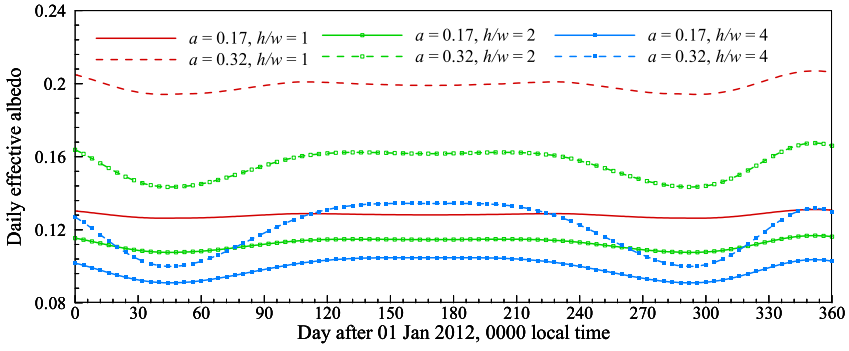

Fig. 12. Seasonal variation of the daily effective albedo for pavements with material albedo of 0.17 and 0.32 in Phoenix urban canyon in year 2012.

area of 5.3×10^{11} m^2 [45], the increase of 0.021–0.070 in average daily effective albedo of urban areas is equivalent to an increase of $4.2 \times 10^{-5} - 1.4 \times 10^{-4}$ in the Earth's albedo. This corresponds to a radiative forcing change of 5.33–17.78 MW and a one-time global CO_2 offset potential of about 2.78–9.33 Gt, which is about 13.9–46.6% of the 20 Gt estimated without considering thermal interactions in the urban canopy. The presented results highlight that the impact of reflective pavements largely depends on the canyon geometry. Moreover, estimating its potential for offsetting greenhouse emission at regional and global scales requires special attention to the heterogeneity of canyon geometry in different cities.

6. Conclusion

This study adopted numerical models with building-environment thermal interactions to evaluate the effect of pavement thermal properties on urban environment at multiple scales. Various thermal properties of pavements were tested, including (1) reflectivity, (2) heat capacity, and (3) thermal conductivity. Results showed that the effect of pavement thermal properties on road and wall surface temperatures was largely modulated by the canyon geometry. Due to radiative shading effect, modifying thermal properties of pavements had a relatively insignificant impact in the urban canyon as compared to that without canopy. For a high-density residential area in Phoenix, different pavements led to similar wall temperatures and building energy consumptions. When applied to different urban facets, same engineering material may have different effects on the building energy efficiency. In terms of outdoor human thermal comfort, due to increased reflected radiation, reflective pavements increased the thermal stress of pedestrians inside the urban canyon considerably, while other pavements did not cause this adverse effect.

With dynamic atmospheric modules and detailed land use land cover information, the online simulation using the WRF-urban modeling system illustrated that modifying pavements had limited impacts on urban land surface temperature and air temperature for the Phoenix metropolitan area. Considering building-environment thermal interactions, a more realistic impact of reflective pavements in terms of CO_2 emission offset and radiative forcing change was estimated. Increase in the daily effective albedo was found to be significantly smaller than the modification of pavement albedo. Depending on the canyon aspect ratio, modifying pavement albedo in the urban canyon led to an offset 13.9–46.6% of the previous estimate, which did not account for building-environment thermal interactions.

Results of numerical simulations suggest that building-environment thermal interactions play a crucial role in determining thermal conditions in urban areas. Accounting thermal interactions in a built environment leads to more realistic and reliable results of numerical simulations. This study provides information regarding how reflective pavements are not an exceptionally effective strategy for mitigating urban heat island and enhancing building energy efficiency as suggested by previous studies that did not consider building-environment thermal interactions.

Acknowledgement

This work is supported by the National Asphalt Pavement Association and US National Science Foundation under grant number CBET-1435881.

References

[1] A.M. Rizwan, L.Y.C. Dennis, C. Liu, A review on the generation, determination and mitigation of Urban Heat Island, J. Environ. Sci. 20 (1) (2008) 120–128.
[2] H. Tran, D. Uchihama, S. Ochi, Y. Yasuoka, Assessment with satellite data of the urban heat island effects in Asian mega cities, Int. J. Appl. Earth Obs. Geoinform. 8 (1) (2006) 34–48.
[3] C. Wang, S.W. Myint, Z. Wang, J. Song, Spatio-temporal modeling of the urban heat island in the Phoenix metropolitan area: land use change implications, Remote Sens. 8 (3) (2016) 185.
[4] H. Akbari, Cooling Our Communities. A Guidebook on Tree Planting and Light-colored Surfacing, Lawrence Berkeley National Laboratory, 2009.
[5] C. Sarrat, A. Lemonsu, V. Masson, D. Guedalia, Impact of urban heat island on regional atmospheric pollution, Atmos. Environ. 40 (10) (2006) 1743–1758.
[6] J. Tan, Y. Zheng, X. Tang, C. Guo, L. Li, G. Song, et al., The urban heat island and its impact on heat waves and human health in Shanghai, Int. J. Biometeorol. 54 (1) (2010) 75–84.
[7] P. Bolund, S. Hunhammar, Ecosystem services in urban areas, Ecol. Econ. 29 (2) (1999) 293–301.
[8] Wong E, Akbari H, Bell R, Cole D. Reducing urban heat islands: compendium of strategies. Environ. Prot. Agency, Retrieved June 2016.
[9] A.J. Arnfield, Two decades of urban climate research: a review of turbulence, exchanges of energy and water, and the urban heat island, Int. J. Climatol. 23 (1) (2003) 1–26.
[10] H. Akbari, R. Levinson, Evolution of cool-roof standards in the US, Adv. Build. Energy Res. 2 (1) (2008) 1–32.
[11] M. Santamouris, Cooling the cities–a review of reflective and green roof mitigation technologies to fight heat island and improve comfort in urban environments, Sol. Energy 103 (2014) 682–703.
[12] J. Yang, Z.-H. Wang, Physical parameterization and sensitivity of urban hydrological models: application to green roof systems, Build. Environ. 75 (2014) 250–263.
[13] J. Yang, Z.-H. Wang, M. Georgescu, F. Chen, M. Tewari, Assessing the impact of enhanced hydrological processes on urban hydrometeorology with application to two cities in contrasting climates, J. Hydrometeorol. 17 (4) (2016) 1031–1047.
[14] H. Akbari, M. Pomerantz, H. Taha, Cool surfaces and shade trees to reduce energy use and improve air quality in urban areas, Sol. Energy 70 (3) (2001) 295–310.
[15] L. Shashua-Bar, M. Hoffman, Vegetation as a climatic component in the design of an urban street: an empirical model for predicting the cooling effect of urban green areas with trees, Energy Build. 31 (3) (2000) 221–235.
[16] Z.-H. Wang, X. Zhao, J. Yang, J. Song, Cooling and energy saving potentials of shade trees and urban lawns in a desert city, Appl. Energy 161 (2016) 437–444.
[17] G. Mihalakakou, M. Santamouris, D. Asimakopoulos, Use of the ground for heat dissipation, Energy 19 (1) (1994) 17–25.
[18] M. Santamouris, Using cool pavements as a mitigation strategy to fight urban heat island—a review of the actual developments, Renew. Sustain. Energy Rev. 26 (2013) 224–240.
[19] K.A. Gray, M.E. Finster, The Urban Heat Island, Photochemical Smog, and Chicago: Local Features of the Problem and Solution, Northwestern University, Department of Civil Engineering, 1999.
[20] J. Yang, Z. Wang, K.E. Kaloush, Unintended Consequences: a Research Synthesis Examining the Use of Reflective Pavements to Mitigate the Urban Heat Island Effect, 2013.
[21] N. Yaghoobian, J. Kleissl, Effect of reflective pavements on building energy use, Urban Clim. 2 (2012) 25–42.
[22] H. Li, Evaluation of Cool Pavement Strategies for Heat Island Mitigation [Ph.D. Thesis], Davis: University of California, 2013, p. 367.
[23] P. Ramamurthy, E. Bou-Zeid, J.A. Smith, Z. Wang, M.L. Baeck, N.Z. Saliendra, et al., Influence of subfacet heterogeneity and material properties on the urban surface energy budget, J. Appl. Meteorol. Climatol. 53 (9) (2014) 2114–2129.
[24] Z.H. Wang, E. Bou-Zeid, J.A. Smith, A coupled energy transport and hydrological model for urban canopies evaluated using a wireless sensor network, Q. J. R. Meteorol. Soc. 139 (675) (2013) 1643–1657.
[25] Z.-H. Wang, E. Bou-Zeid, J.A. Smith, A spatially-analytical scheme for surface temperatures and conductive heat fluxes in urban canopy models, Bound. Layer Meteorol. 138 (2) (2011) 171–193.
[26] J. Song, Z.-H. Wang, Impacts of mesic and xeric urban vegetation on outdoor thermal comfort and microclimate in Phoenix, AZ, Build. Environ. 94 (2015) 558–568.
[27] M.J. Best, Representing urban areas within operational numerical weather prediction models, Bound. Layer Meteorol. 114 (1) (2005) 91–109.
[28] F. Chen, H. Kusaka, R. Bornstein, J. Ching, C.S.B. Grimmond, S. Grossman-Clarke, et al., The integrated WRF/urban modelling system: development, evaluation, and applications to urban environmental problems, Int. J. Climatol. 31 (2) (2011) 273–288.
[29] A. Martilli, A. Clappier, M. Rotach, An urban surface exchange parameterisation for mesoscale models, Bound. Layer Meteorol. 104 (2) (2002) 261–304.
[30] F. Salamanca, A. Martilli, M. Tewari, F. Chen, A study of the urban boundary layer using different urban parameterizations and high-resolution urban canopy parameters with WRF, J. Appl. Meteorol. Climatol. 50 (5) (2011) 1107–1128.
[31] S. Miao, F. Chen, Formation of horizontal convective rolls in urban areas, Atmos. Res. 89 (3) (2008) 298–304.
[32] H. Kusaka, F. Chen, M. Tewari, J. Dudhia, D.O. Gill, M.G. Duda, et al., Numerical simulation of Urban Heat Island effect by the WRF Model with 4-km grid

increment: an inter-comparison study between the urban canopy model and slab model, J. Meteorol. Soc. Jpn. B 90 (2012) 33–45.
[33] J.A. Fry, G. Xian, S. Jin, J.A. Dewitz, C.G. Homer, Y. LIMIN, et al., Completion of the 2006 national land cover database for the conterminous United States, Photogramm. Eng. Remote Sens. 77 (9) (2011) 858–864.
[34] F. Ali-Toudert, H. Mayer, Numerical study on the effects of aspect ratio and orientation of an urban street canyon on outdoor thermal comfort in hot and dry climate, Build. Environ. 41 (2) (2006) 94–108.
[35] J. Song, Z.-H. Wang, Interfacing the urban land–atmosphere system through coupled urban canopy and atmospheric models, Bound. Layer Meteorol. (2014) 1–22.
[36] J. Yang, Z.-H. Wang, Optimizing urban irrigation schemes for the trade-off between energy and water consumption, Energy Build. 107 (2015) 335–344.
[37] J. Yang, Z.-H. Wang, F. Chen, S. Miao, M. Tewari, J. Voogt, et al., Enhancing hydrologic modelling in the coupled weather research and forecasting–urban modelling system, Bound. Layer Meteorol. 155 (1) (2015) 87–109.
[38] U.S. Department of Energy. Energy Saver: Thermostats. http://energy.gov/energysaver/thermostats. Retrieved Aug 8, 2016.
[39] J. Yang, Z.-H. Wang, K.E. Kaloush, Environmental impacts of reflective materials: is high albedo a 'silver bullet'for mitigating urban heat island? Renew. Sustain. Energy Rev. 47 (2015) 830–843.
[40] A. Brazel, N. Selover, R. Vose, G. Heisler, The tale of two climates-Baltimore and Phoenix urban LTER sites, Clim. Res. 15 (2) (2000) 123–135.
[41] J.A. Patz, D. Campbell-Lendrum, T. Holloway, J.A. Foley, Impact of regional climate change on human health, Nature 438 (7066) (2005) 310–317.
[42] A.K. Mishra, M. Ramgopal, Field studies on human thermal comfort—an overview, Build. Environ. 64 (2013) 94–106.
[43] Givoni B. Estimation of the Effect of Climate on Man: Development of a New Thermal Index: Technion-IIT, Building Research Station, 1963.
[44] D. Pearlmutter, P. Berliner, E. Shaviv, Physical modeling of pedestrian energy exchange within the urban canopy, Build. Environ. 41 (6) (2006) 783–795.
[45] H. Akbari, S. Menon, A. Rosenfeld, Global cooling: increasing world-wide urban albedos to offset CO2, Clim. Change 94 (3–4) (2009) 275–286.